JMEPEG (2012) 21:1363–1373
DOI: 10.1007/s11665-011-0007-0

1059-9495/$19.00

Effect of Some Oxadiazole Derivatives on the Corrosion Inhibition of Brass in Natural Seawater

X. Joseph Raj and N. Rajendran

(Submitted November 17, 2010; in revised form June 20, 2011)

The electrochemical behavior of brass in natural seawater in the absence and presence of oxadiazole derivatives, namely 2,5-bis-(4-aminophenyl)-1,3,4-oxadiazole (BAPOD), 2,5-bis-(4-bromophenyl)-1,3,4-oxadiazole (BBPOD), 2,5-diphenyl-1,3,4-oxadiazole (DPOD), and 2,5-bis-(4-nitrophenyl)-1,3,4-oxadiazole (BNPOD) has been investigated by potentiodynamic polarization and electrochemical impedance spectroscopy (EIS). The inhibition efficiency of the inhibitors was also evaluated at different temperatures. The inhibition efficiency was found to increase with increase in concentration of the inhibitors but decrease with rise in temperature for all the inhibitors except BNPOD. Inductively coupled plasma atomic emission spectroscopic (ICP-AES) analysis confirmed that dezincification was minimized to a greater extent in the presence of the inhibitors. Scanning electron microscopy (SEM), energy dispersive x-ray analysis (EDX) and Fourier transform infrared spectroscopy (FT-IR) observations of the brass surface confirmed the existence of an adsorbed film.

Keywords brass, corrosion inhibition, impedance spectroscopy, oxadiazole derivatives, potentiodynamic polarization

1. Introduction

Copper and its alloys are widely used in marine environments due to their corrosion resistance, mechanical workability, anti-biofouling, excellent electrical and thermal conductivities. Brass is used extensively in marine applications such as heat exchanger tubes, desalination and shipboard condensers, power plant condensers and petrochemical heat exchangers (Ref 1, 2). Both scale and corrosion products have negative effects on heat transfer and cause a decrease in the heating efficiency of the equipment. In a marine environment, chloride ions form strong complexes with Cu ions and weaker complexes with Zn ions, which affects the equilibrium potentials which in turn leads to the dissolution of the Cu and Zn components of the alloy. Consequently, chloride ions are bound to affect the selective dissolution behavior of the alloy. The selective corrosion of alloys involves preferential dissolution of the active component of the alloy leaving behind a weak surface which is enriched in the nobler component. The process leads to serious deterioration of the surface and mechanical properties of the remaining alloy and hence increases the risk of corrosion failures, which may be costly or catastrophic. The dezincification of brass is one of the more recognized forms of this phenomenon.

In order to overcome these shortcomings, inhibitors are used to prevent corrosion of copper and its alloys in aqueous environments (Ref 3-5). Many organic compounds, specially containing polar groups and/or substituted heterocycle including nitrogen, sulfur, and oxygen in their structures have been reported to prevent dezincification. The inhibiting action of these organic compounds is usually attributed to the formation of donor-acceptor surface complexes between the free or π electrons of an inhibitor and the vacant *d*-orbital of a metal interaction with the copper surface via adsorption (Ref 6), and to their molecular structure (Ref 7). Recently, it has been shown that the adsorption of organic inhibitors mainly depends on physicochemical and electronic properties of the molecule, related to their functional groups, steric effects, electron density of donor atoms, and the π-orbital character of donating electrons (Ref 8). We have extensively carried out the corrosion inhibition effect of benzotriazole derivatives for brass in seawater (Ref 9-13). Of the various nitrogeneous compounds studied as inhibitors, BTA and its derivatives are excellent corrosion inhibitors for copper and its alloys in a wide range of media, but the disadvantage of BTA is its toxicity. Moreover, data regarding the use of *N*-heterocyclic compounds such as oxadiazole derivatives are not so plentiful. Our research is aimed at making compounds with low toxicity and good inhibition efficiency against brass corrosion. In the extension of this work, we have made an attempt to use some of the oxadiazole derivatives, namely 2,5-bis-(4-aminophenyl)-1,3,4-oxadiazole (BAPOD), 2,5-bis-(4-bromophenyl)-1,3,4-oxadiazole (BBPOD), 2,5-diphenyl-1,3,4-oxadiazole (DPOD), and 2,5-bis-(4-nitrophenyl)-1,3,4-oxadiazole (BNPOD) for the prevention of brass corrosion in natural seawater.

2. Experimental Section

2.1 Materials

BAPOD, BBPOD, DPOD, and BNPOD (Sigma-Aldrich, 98%) and absolute ethanol (C_2H_5OH, Fischer, 99.9%) were used as received. The structures of oxadiazole derivatives are shown in Fig. 1. The electrolyte used was the natural sea water

X. Joseph Raj and **N. Rajendran**, Department of Chemistry, Anna University, Chennai 600 025, India. Contact e-mail: nrajendran@annauniv.edu.

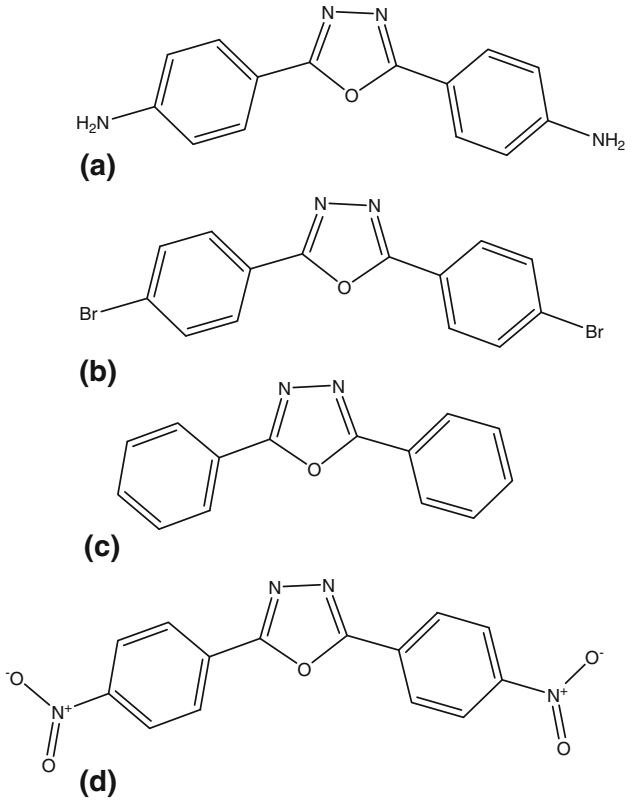

Fig. 1 The structure of investigated organic inhibitors (a) 2,5-bis-(4-aminophenyl)-1,3,4-oxadiazole (BAPOD), (b) 2,5-bis-(4-bromophenyl)-1,3,4-oxadiazole (BBPOD), (c) 2,5-diphenyl-1,3,4-oxadiazole (DPOD), and (d) 2,5-bis-(4-nitrophenyl)-1,3,4-oxadiazole (BNPOD)

collected in a sterilized brown flask at Eliot beach on the southern coast of Chennai, India. The working electrode used for the study having the chemical composition as wt.% 65.3 Cu, 34.44 Zn, 0.1385 Fe, and 0.0635 Sn. The brass specimens were polished mechanically with different grades of silicon carbide papers (400-1200) and washed with double distilled water. Further the samples were degreased with acetone using ultrasonicator and thoroughly washed with double distilled water and dried in air. Different concentrations of the inhibitors were added into the electrolyte to find out the optimum concentration of the inhibitor.

2.2 Potentiodynamic Polarization Studies

An electrochemical cell with a three electrode assembly was used to study the electrochemical measurements. Brass specimens with exposed area of 0.28 cm^2, a platinum foil of 1 cm^2 area and silver/silver chloride Ag/AgCl in saturated KCl (Advance-Tech Controls Pvt. Ltd, India) were used as working, counter and reference electrodes, respectively. The polarization experiments were carried out using the Potetiostat/Galvanostat (Model PGSTAT 12, AUTOLAB, the Netherlands B.V.) controlled by a personal computer with dedicated software (GPES version 4.9.005). The working electrode was immersed in natural sea water in the presence and absence of different concentrations of the inhibitors to which a current of -1.0 mA cm^{-2} was applied for 15 min to reduce oxides and then allowed to stabilize for 30 min. The polarization experiments were carried out for brass specimen at a scan rate of 1 mV/s in the presence and absence of inhibitors in natural sea water. In order to test the reproducibility of the results, the experiments were performed in triplicate.

2.3 Electrochemical Impedance Spectroscopy

Electrochemical impedance measurements were conducted using a potentiostat/galvanostat (Model PGSTAT 12, AUTOLAB (ECO CHEMIE B.V., Netherlands), the Netherlands B.V.) with frequency response analyzer (FRA). The impedance measurements were carried out at an open circuit potential (OCP), after 30 min immersion of the brass electrode in the corrosive medium. The impedance data were acquired in the frequency range of 100 kHz-50 mHz with an AC voltage amplitude of 10 mV.

2.4 Analysis of FT-IR Spectroscopy

The film surface formed on the brass in the presence of the inhibitor was collected by scrapping from the surface of the alloy for spectral analysis with Fourier transform infrared spectroscopy (FT-IR). FT-IR spectra were recorded between 4000 and 400 cm^{-1} using 12 scans with a resolution of 1 cm^{-1} using a Perkin-Elmer Model 577 spectrometer.

2.5 Inductively Coupled Plasma Atomic Emission Spectroscopy

The concentration of copper and zinc in the electrolytes, after the polarization experiments in the presence and absence of 10^{-2} M oxadiazole derivatives, were determined by inductively coupled plasma atomic emission spectroscopy (ICPAES). An ICPAES (ARCOS from M/s. Spectro, Germany) was used to measure the amount of dissolution of zinc and copper from the brass surface. The dezincification factor (z) was calculated using the equation (Ref 14)

$$z = \frac{[C_{Zn}/C_{Cu}]_{sol}}{[C_{Zn}/C_{Cu}]_{alloy}}, \quad \text{(Eq 1)}$$

where $[C_{Zn}/C_{Cu}]_{sol}$ and $[C_{Zn}/C_{Cu}]_{alloy}$ are the ratios between the concentrations of zinc and copper in the solution and in the alloy, respectively.

2.6 SEM and EDX Investigations

The brass surface was prepared for SEM and EDX studies by keeping the specimens for an hour in the electrolyte with and without the optimum concentrations of the inhibitors. The brass specimens were then washed with distilled water, dried, and analyzed using SEM/EDX. A Philips model XL30SFEG scanning electron microscope with an energy dispersive x-ray analyzer attached was used for surface analysis.

3. Results and Discussion

3.1 Potentiodynamic Polarization Measurements

Potentiodynamic polarization measurements for brass in natural seawater in the presence and absence of BAPOD, BBPOD, DPOD, and BNPOD were carried out, respectively, and are shown in the Fig. 2(a-d). The corrosion current density

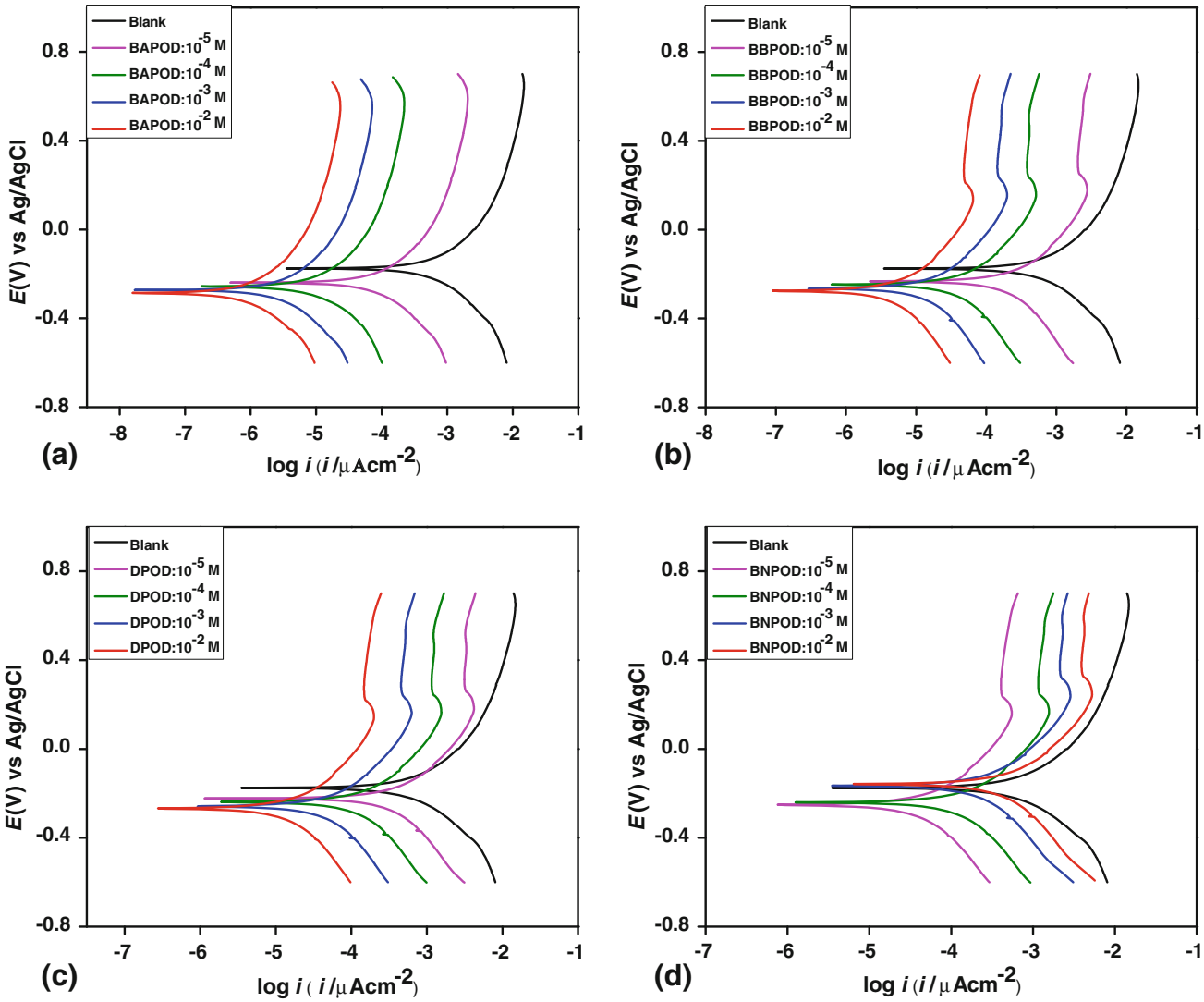

Fig. 2 Potentiodynamic polarization curves for brass in natural seawater in the absence and presence of various concentrations of (a) BAPOD, (b) BBPOD, (c) DPOD, and (d) BNPOD

(I_{corr}), corrosion potential (E_{corr}), anodic β_a and cathodic β_c slopes, corrosion rate were obtained by extrapolating the cathodic and anodic regions of the Tafel plots and are presented in Table 1. It is known from the polarization curves, both anodic and cathodic reactions of brass corrosion were suppressed in the presence of the oxadiazole derivatives in natural seawater and suppression effect increases with the increase in the concentration of BAPOD, BBPOD, and DPOD. The optimum concentration used was 10^{-3} M for BAPOD, BBPOD, and DPOD. In contrast, the optimum concentration used was 10^{-4} M for BNPOD. It is evident from the table that both corrosion current densities I_{corr} and corrosion rate decreased significantly with increase in inhibitor concentration, except in the case of BNPOD. The highest inhibiting effect was observed with BAPOD. In all the cases, corrosion inhibition is under mixed control. The inhibiting effect of BAPOD, BBPOD, and DPOD were in the same efficiency range and their E_{corr} was shifted most cathodically. The current density decreases even at the lowest inhibitor concentration with efficiencies of 40-74%. For instance, the concentration of 10^{-2} M, the inhibition efficiency of BAPOD, BBPOD, and DPOD exhibited 86, 85, and 82%, respectively.

However, the inhibition efficiency decreases with increase in concentration of the BNPOD, which may be due to the electron donating group (Ref 15). Interestingly, nitro groups attached to the phenyl ring shows opposite effects. However, BNPOD exhibited maximum inhibition efficiency of 74% only at the lower concentration 10^{-5} M. The corrosion inhibition efficiency of BAPOD, BBPOD, and DPOD improved with increase in concentration while that of BNPOD decreases. Moreover, the corrosion potential was shifted anodically when BNPOD was used due to large decrease in the β_c, cathodic slopes which showed that the inhibiting effect has decreased (Ref 16). It is likely that at higher concentration of 10^{-2} M BNPOD showed insignificant effect due to the presence of electron withdrawing nitro group. The order of their efficiency is BAPOD $>$ BBPOD $>$ DPOD $\gg$ BNPOD. The lowest corrosion rate and highest inhibition effect are evident for BAPOD.

3.2 Electrochemical Impedance Spectroscopy

Electrochemical impedance spectroscopic measurements were carried out in order to understand the mechanism taking

Table 1 Tafel polarization parameters for the corrosion of brass in natural seawater in the absence and presence of different concentration (10^{-5}-10^{-2} M) of BAPOD, BBPOD, DPOD, and BNPOD

Compound	Conc., M	E_{corr}, mV	I_{corr}, μA/cm^2	β_c, mV/dec	β_a, mV/dec	CR, mm/year × 10^{-3}	Surface coverage, θ	IE, %
Blank	...	−176	2.85	42	50	140	...	...
BAPOD	10^{-5}	−239	1.63	58	66	80	0.43	43
	10^{-4}	−256	0.78	71	78	38	0.73	73
	10^{-3}	−273	0.39	85	91	19	0.86	86
	10^{-2}	−286	0.38	82	93	19	0.87	87
BBPOD	10^{-5}	−232	1.68	56	59	82	0.41	41
	10^{-4}	−248	0.81	67	74	40	0.72	72
	10^{-3}	−266	0.44	79	83	21	0.85	85
	10^{-2}	−276	0.43	81	85	21	0.85	85
DPOD	10^{-5}	−223	1.71	54	63	83	0.40	40
	10^{-4}	−238	0.84	64	67	41	0.71	71
	10^{-3}	−259	0.51	72	75	25	0.82	82
	10^{-2}	−267	0.49	74	78	24	0.83	83
BNPOD	10^{-5}	−251	0.74	73	74	36	0.73	74
	10^{-4}	−241	0.76	73	82	36	0.73	73
	10^{-3}	−166	2.32	41	42	114	0.19	19
	10^{-2}	−158	2.68	39	41	136	0.06	6

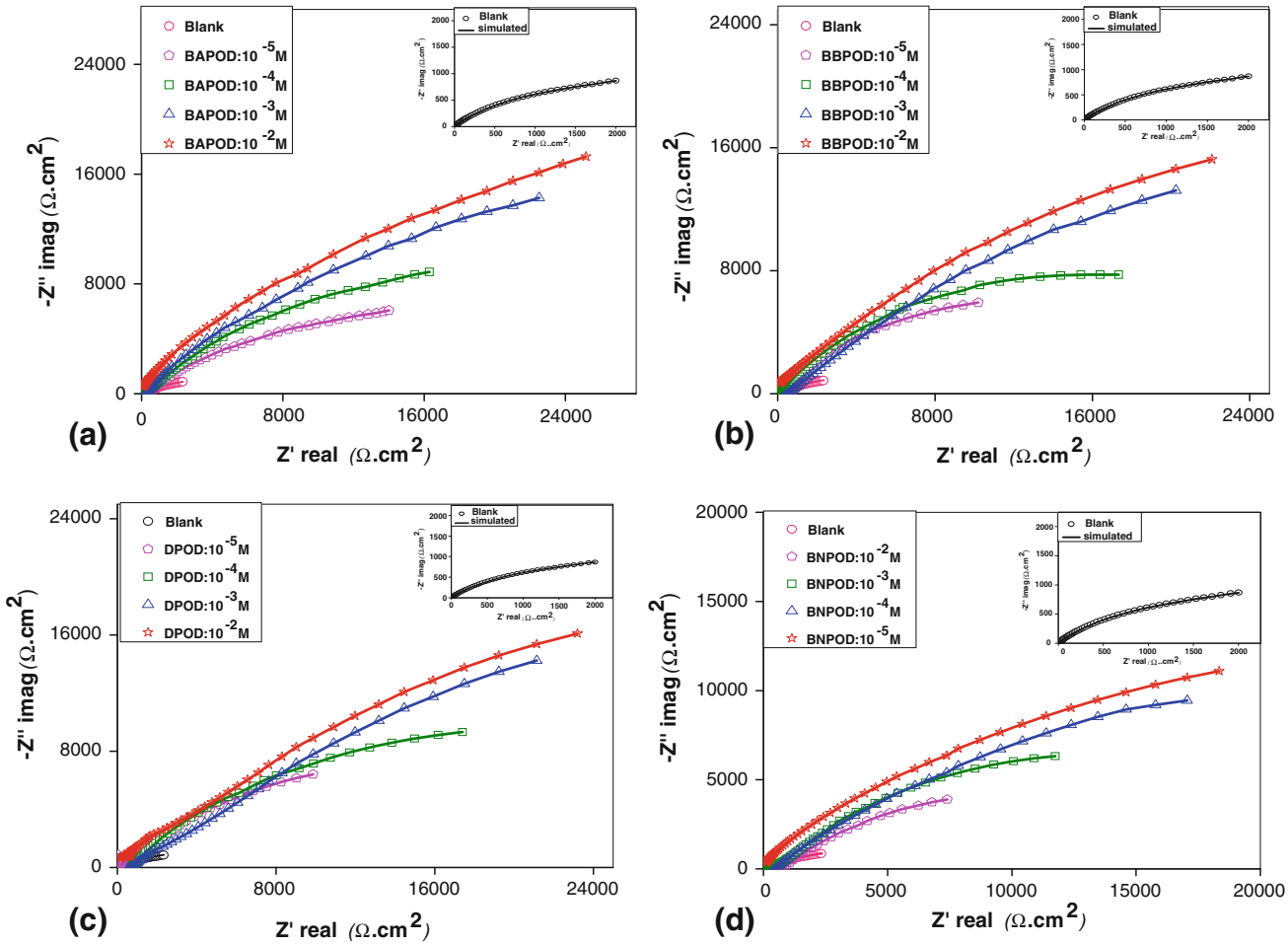

Fig. 3 Nyquist plots of brass in natural seawater in the absence and presence of different concentrations of oxadiazole derivatives; (a) BAPOD, (b) BBPOD, (c) DPOD, and (d) BNPOD

place at the brass surface. The Nyquist plots of brass in natural seawater in the presence and absence of BAPOD, BBPOD, DPOD, and BNPOD are shown in Fig. 3. The Nyquist plots are significantly changed on addition of inhibitors, the impedance of the inhibited system increased with inhibitor concentration. The parameters obtained by fitting the equivalent circuit and the

Table 2 Electrochemical parameter values for brass corrosion calculated by nonlinear least square regression of the impedance data using the electrical equivalent circuits

Inhibitor conc., M	R_s, Ω cm^2	R_f, Ω cm^2	C_f, μF/cm^2	n_f	R_{ct}, Ω cm^2	C_{dl}, μF/cm^2	n_{dl}	R_F, Ω cm^2	C_F, μF/cm^2	n_F	IE, %
Blank	46	···	···	···	1250	145	0.68	1375	75	0.67	···
BAPOD											
10^{-5}	195	1240	28	0.90	1650	29	0.89	1700	28	0.89	43
10^{-4}	237	2550	17	0.94	3400	17	0.92	3550	15	0.93	72
10^{-3}	294	5150	15	0.96	6790	15	0.94	7140	13	0.95	86
10^{-2}	392	5390	12	0.97	7160	12	0.95	7470	12	0.96	87
BBPOD											
10^{-5}	188	1210	33	0.90	1620	35	0.88	1670	33	0.89	42
10^{-4}	220	2550	19	0.93	3400	20	0.91	3550	17	0.92	72
10^{-3}	282	5150	16	0.95	6790	16	0.93	7140	15	0.94	85
10^{-2}	376	5390	12	0.96	7160	13	0.94	7470	12	0.95	85
DPOD											
10^{-5}	164	1180	38	0.89	1575	39	0.87	1620	37	0.88	40
10^{-4}	198	2400	22	0.92	3125	23	0.90	3270	22	0.91	70
10^{-3}	265	4090	16	0.94	5370	17	0.92	5640	16	0.93	83
10^{-2}	334	4180	13	0.95	5465	13	0.93	5750	13	0.94	83
BNPOD											
10^{-5}	218	2670	15	0.92	3660	16	0.90	3770	14	0.88	74
10^{-4}	216	2615	16	0.90	3610	17	0.88	3715	16	0.89	74
10^{-3}	75	480	48	0.75	1320	50	0.73	1410	47	0.74	18
10^{-2}	32	220	67	0.70	1170	67	0.69	1245	66	0.68	6

$R_p = R_f + R_{ct} + R_F$; R_S—electrolyte resistance, R_{ct}—charge-transfer resistance, C_{dl}—charge-transfer capacitance, R_F—Faradic resistance, C_F—Faradic capacitance, R_f—film resistance, C_f—capacitance due to surface film and n_f, n_{dl}, and n_F—coefficients representing the depressed characteristic of the three capacitive loops

calculated inhibition efficiency are listed in Table 2. The percentage inhibition efficiency (IE %) of oxadiazole derivatives on brass was calculated using the equation:

$$\text{IE } (\%) = \frac{R_{p\,(inh)} - R_p}{R_{p\,(inh)}} \times 100, \qquad \text{(Eq 2)}$$

where $R_{P(inh)}$ and R_P are polarization resistance in the presence and absence of inhibitors in electrolytes, respectively (Ref 17). The value of R_P is calculated as the sum of R_f, R_{ct}, and R_F, i.e., $R_P = R_f + R_{ct} + R_F$. Similarly, $R_P° = R_{ct} + R_F$.

The impedance spectra in the presence inhibitors showed a capacitive behavior throughout the measured frequency range. The impedance spectra in the presence of inhibitors can be modeled by three capacitive loops and in the absence of inhibitors, it can be modeled using two capacitive loops (Ref 18, 19) and the fitting parameters were performed by a nonlinear least square method, which is shown in Fig. 4(a, b). In these equivalent circuits, R_s is the solution resistance; R_f and C_f denote the resistance and capacitance corresponding to the surface film, R_{ct} and C_{dl} represent the charge-transfer resistance and the double layer capacitance; R_F and C_F indicate the faradaic resistance and faradic capacitance, respectively. Corrosion product accumulated at the electrode surface present some amount of reversibility of the redox and/or charge; the exponents n_f, n_{dl}, and n_F are the depressed features in Nyquist plot.

The most pronounced and highest charge-transfer resistance was observed for BAPOD while BNPOD showed an insignificant change. R_{ct} increases with concentration for all inhibitors except BNPOD. Table 2 indicated that by increasing the concentration of oxadiazole derivatives, C_{dl} values tend to decrease and the inhibition efficiency increases. The decrease in C_{dl}, which result from local dielectric constant decrease and/or

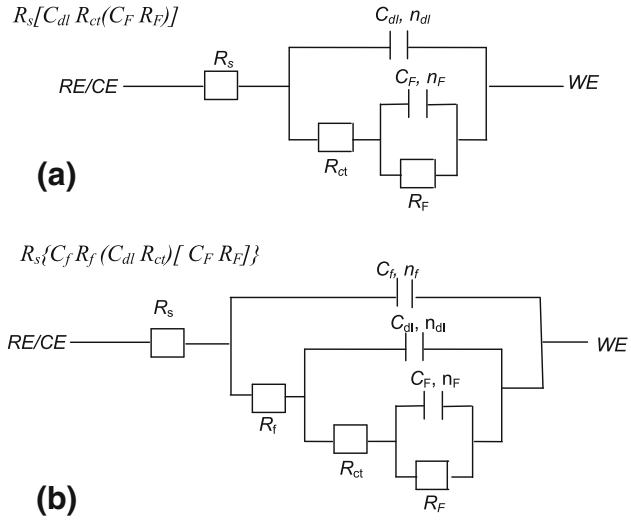

Fig. 4 The equivalent electrical circuits used to fit the experimental data for the brass in natural seawater in the absence (a) and presence of BAPOD, BBPOD, DPOD, and BNPOD (b) compounds: (a) $R_s[C_{dl}\ R_{ct}(C_F\ R_F)]$, (b) $R_s\{C_fR_f\ (C_{dl}\ R_{ct})[C_F\ R_F]\}$

an increase in the thickness of the electrical double layer, suggest that these molecules act by adsorption on the metal/solution interface.

It is clear that R_{ct} increases and C_{dl} decreases as the inhibitor concentration increases. The decrease in C_{dl} could be attributed to the adsorption of the inhibitor, forming a protective adsorption layer (Ref 20). A high charge-transfer resistance is associated with a slower corroding system (Ref 21). Furthermore, better protection provided by an inhibitor can be associated

with a decrease in capacitance of the metal. It is clear that the highest values of R_{ct} observed for BAPOD followed by BBPOD and DPOD, suggesting their enhanced inhibitor performance. In the presence of BNPOD, the R_{ct} decreased and the C_{dl} increased notably, approaching the values for the uninhibited solution. The reason for that might be diffusion, along with desorption of BNPOD with partial adsorption of water or electrochemical reduction of nitro group (Ref 22).

The faradaic resistance that linked to the redox reaction involving corrosion process increases and the faradaic capacitance decreases simultaneously with increase in concentration of all the inhibitors except BNPOD. From this it can be concluded that the corrosion products are less susceptible to redox process with increase in concentration of the inhibitors except BNPOD and give better protection efficiency to brass surface. The decrease in faradaic resistance and increase in faradaic capacitance with increase in concentration of the BNPOD may be due to the presence of electron withdrawing nitro group leading to the desorption of BNPOD.

It can be seen that R_f values increased and C_f values decreased for all inhibitors. It is attributed to the increase of true surface area which is partly due to the formation of the corrosion products and also to the roughening of electrode surface. The value of resistance and capacitance involved here are very high and it may be related to the redox process taking place at the electrode surface. The R_F increased and C_F decreased except BNPOD, may be due to the blocking of the surface.

The inhibition efficiency increased with increase in concentration and a maximum inhibition efficiency of 86% was observed for 10^{-2} M BAPOD. The maximum IE% for 10^{-2} M BBPOD and DPOD were 85 and 82%, respectively. The maximum inhibition efficiency for BNPOD at 10^{-5} M was found to be 74%, whereas at 10^{-2} M it was found to be 5%. The investigations proved that the effectiveness of the oxadiazole derivatives as corrosion inhibitors depends on their molecular structure, particularly on their molecular size and electronic effects of the substituent in the molecule. The IE% calculated from electrochemical impedance spectroscopy (EIS) show the same trend as those estimated from polarization measurements, i.e., polarization measurements and EIS study complement each other well.

3.3 Effect of Temperature

Temperature has a great effect on the rate of electrochemical corrosion of a metal. Temperature can modify the interaction between the brass electrode and the natural seawater media with and without the inhibitors. Potentiodynamic polarization curves for brass in natural seawater at different temperatures (303-343 K) in the presence and absence of 10^{-3} M of BAPOD, BBPOD, and DPOD and 10^{-4} M of BNPOD are shown in Fig. 5. The corrosion current density increased and the inhibition efficiency decreased with the increase of temperature both in the absence and presence of inhibitors. Thus, both corrosion current density and inhibition efficiency of the inhibitors are temperature-dependant in natural seawater. The decrease in inhibition efficiency with increase in temperature was due to the desorption of the inhibitor from the brass surface. The increase in temperature slightly shifts E_{corr} in the positive direction and enhances both cathodic and anodic current densities. This may be attributed to the fact that an increase in temperature usually accelerates corrosive processes, giving rise to higher metal dissolution rates and a possible shift of the adsorption-desorption equilibrium toward desorption. This, as well as roughening of the metal surface as a result of enhanced corrosion, may also reduce the ability of the inhibitor to be adsorbed on the metal surface. The observed decrease in the strength of adsorption at higher temperatures suggested that the chemisorptions may be the main type of adsorption of oxadiazole derivatives. The decrease in inhibition efficiency with increasing temperature may be due to the increase in desorption of BAPOD, BBPOD, DPOD, and BNPOD (Ref 23).

3.4 Inductively Coupled Plasma Atomic Emission Spectroscopic Analysis

The concentrations of copper and zinc in solutions containing 10^{-3} M of the oxadiazole derivatives after polarization measurements were determined from inductively coupled plasma atomic emission spectroscopic (ICP-AES) analysis. The dezincification (z) factors for brass in the absence and presence of 10^{-3} M of BAPOD, BBPOD, DPOD, and 10^{-4} M of BNPOD in natural seawater were calculated from the ICP-AES data and the results are shown in Table 3. The results showed that both copper and zinc were present in the electrolyte in very small quantities and the copper to zinc ratio was found to be lower than that of the bulk alloy. This is due to the surface barrier arising out of the growth of surface film of inhibitor on the metal surface as well as the corrosion product Cu_2O and ZnO. It is clear from the table that dezincification was much higher in the absence of inhibitors, while dezincification was much lower in the presence of 10^{-3} M concentration of BAPOD, BBPOD, and DPOD. On the other hand, in the presence of BNPOD, the dezincification factor was predominated on increasing the concentration. Much higher amounts of copper and zinc for BNPOD than for BAPOD were found, suggesting dissolution of copper and zinc (i.e., more rapid corrosion) even in the presence of BNPOD. This indicated that the BAPOD, BBPOD, and DPOD were able to minimize the dissolution of both zinc and copper. These values correlate with the corrosion rate and inhibition efficiency obtained by electrochemical methods.

3.5 FT-IR Spectroscopic Analysis

The FT-IR spectra obtained for surface films of BAPOD, BBPOD, DPOD, and BNPOD after adsorption of the inhibitors on brass are presented in Fig. 6(a-d). The bands at 1412, 1492, 1439, and 1407 cm^{-1} were assigned to the stretching vibrations of the C=N group in the ring for the surface films of BAPOD, BBPOD, DPOD, and BNPOD compounds, respectively. This indicated that there was a coordination of the ring to the metal surface. The ring N-N stretching vibrations for the compounds BAPOD, BBPOD, DPOD, and BNPOD were observed at 1012, 1020, 1011, and 1071 cm^{-1}, respectively. The strong bands were observed at 1579, 1472, 1552, and 1596 cm^{-1} are due to the C=C stretching vibration of BAPOD, BBPOD, DPOD, and BNPOD, respectively. The ring C–O vibration for the compounds BAPOD, BBPOD, DPOD, and BNPOD are observed, respectively, at 1058, 1091, 1098, and 1090 cm^{-1}. The N-H stretching vibration due to the surface films of BAPOD at 3454 cm^{-1} indicated the complex formation with metal involving the NH_2 group. The strong band at 1604 cm^{-1} was attributed to the (N H) in-plane bending vibrations of the surface films of the BAPOD compound. The strong band at 527 cm^{-1} for BBPOD was assigned to C-Br stretching

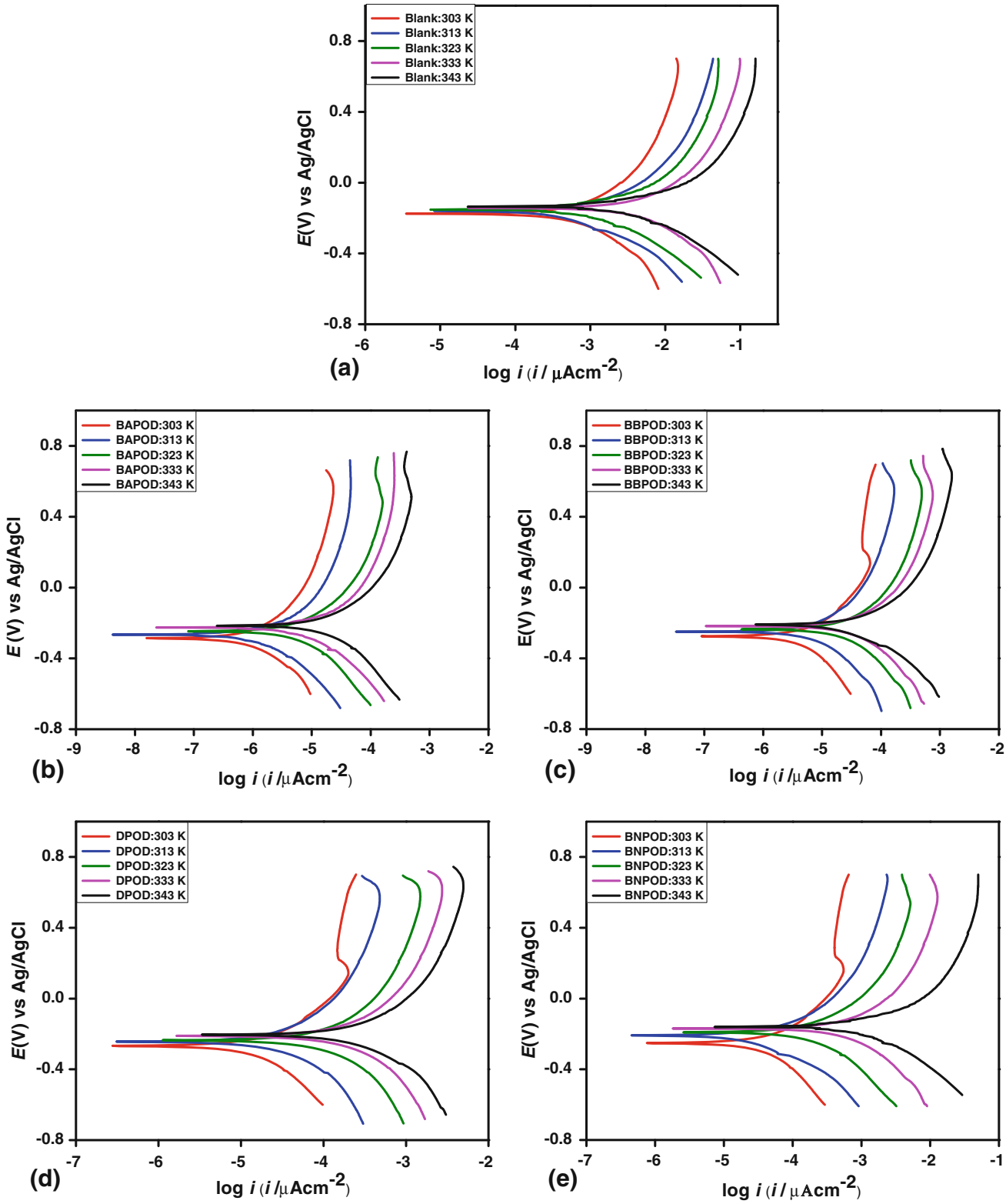

Fig. 5 Effect of temperature on the potentiodynamic polarization curves for brass in natural seawater in the absence and presence of optimum concentrations of (a) BAPOD (10^{-3} M), (b) BBPOD (10^{-3} M), (c) DPOD (10^{-3} M), and (d) BNPOD (10^{-4} M) at the range of 303-343 K

vibrations. The strong band at 1642 cm^{-1} was due to the presence of N=O group. The symmetrical and asymmetrical C-NO_2 stretching vibrations of BNPOD were observed at 1342 and 1510 cm^{-1}, respectively, and the corresponding bands for surface films of BNPOD were shifted to higher region.

3.6 SEM and EDX Analysis

The SEM and EDX experiments were carried out in order to verify the adsorption of oxadiazole derivatives on brass surface. The SEM micrograph obtained for the brass surface in the

Table 3 Quantum chemical parameters of BAPOD, BBPOD, DPOD, and BNPOD

Inhibitors	Solution analysis		Dezincification factor (z)	Percent inhibition	
	Cu/10^{-6} M	Zn/10^{-6} M		Cu	Zn
Blank	0.75	17.25	42.7	...	...
BAPOD	0.12	1.98	30.6	84	89
BBPOD	0.13	2.26	32.3	83	87
DPOD	0.15	2.65	32.8	80	85
BNPOD	0.71	16.10	42.1	5	7

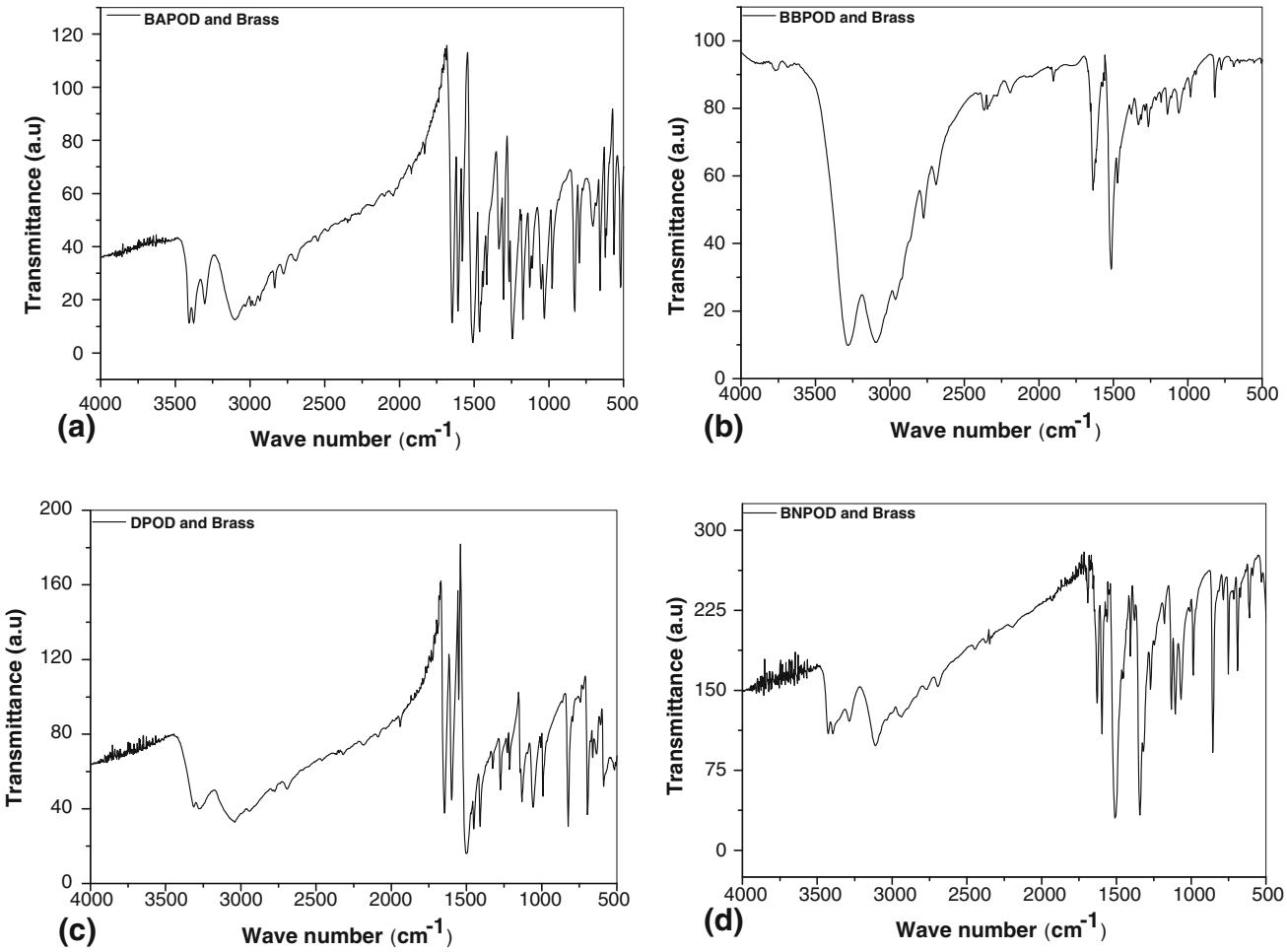

Fig. 6 The FT-IR spectra after adsorption of the inhibitors BAPOD, BBPOD, DPOD, and BNPOD on brass

absence and presence of optimum concentration of the inhibitors in natural seawater are shown in Fig. 7(a-e). The brass surface in the absence of inhibitors exhibited a highly corroded surface with pits and cracks. This is due to the attack of brass surface with aggressive chloride ions in natural seawater. However, in the presence of BAPOD, BBPOD, DPOD, and BNPOD, the brass surface could be observed with a thin layer of the inhibitor molecules, giving protection against corrosion. The inhibited brass surface was smoother than the uninhibited surface indicating the presence of a protective layer of adsorbed inhibitor preventing chloride attack in natural seawater. This protection ability was due to the formation of copper and zinc complexes of BAPOD, BBPOD, DPOD, and BNPOD over the brass surface against corrosion. The formed surface film has higher stability and low permeability in aggressive solution than uninhibited brass surface. Hence, they show an enhanced surface properties, which seemed to provide corrosion protection to the brass beneath them by restricting the mass transfer of reactants and products between the bulk solution and the brass surface.

The EDX spectra were used to determine the elements present on the brass surface before and after exposure to the inhibitor solution. It is also important to notice the existence of the nitrogen, oxygen, and sulfur atoms in the EDX spectra of BAPOD, BBPOD, DPOD, and BNPOD. Figure 8(a-e) shows the EDX spectra for the samples in the absence and presence of optimum concentrations of inhibitors. In the absence of inhibitors, the EDX spectra confirmed the existence of chlorine

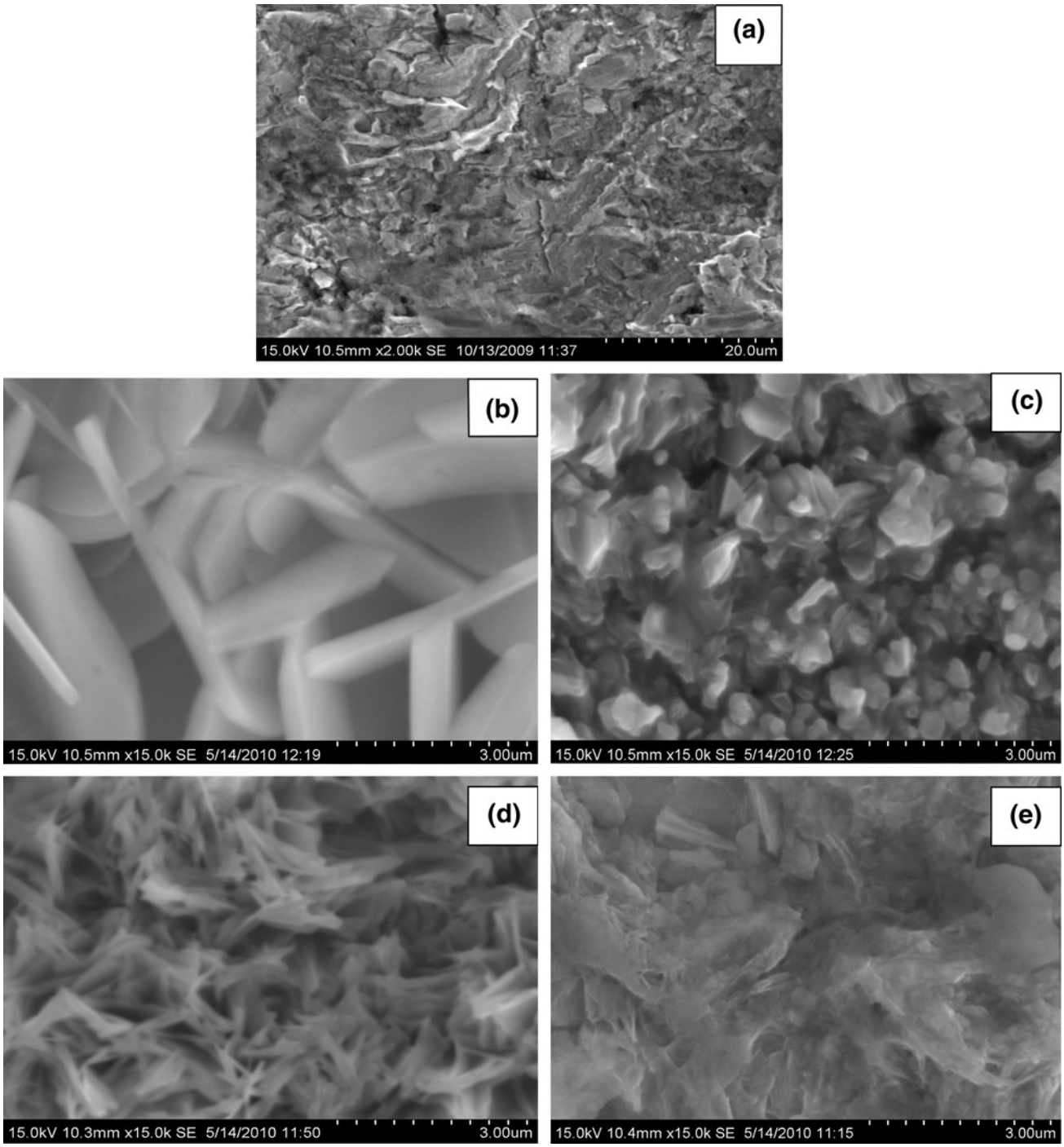

Fig. 7 SEM images of brass (a) blank, (b) BAPOD, (c) BBPOD, (d) DPOD, and (e) BNPOD

and oxygen along with copper and zinc due to the formation of Cu_2O and $CuCl_2^-$ complex, which showed that the passive film contained only by Cu_2O and $CuCl_2^-$ (Ref 24). This indicated that the inhibitor molecules were able to protect the brass surface against corrosion.

3.7 Mechanism of Corrosion Inhibition

The inhibitor molecules can be adsorbed onto the metal surface through electron transfer from the adsorbed species to the vacant *d*-orbital in the metal to form a coordinate type link. It is well known that the metal has coordination affinity toward nitrogen, sulfur, and oxygen-bearing ligands. The studied compounds contain two iminic group (–C=N) and one C–O group of oxadiazole ring besides the bis-(4-aminophenyl) group in BAPOD, bis-(4-bromophenyl) group in BBPOD, diphenyl group in DPOD, and bis-(4-nitrophenyl)-group in BNPOD, respectively. The unshared electron pairs on N and O are capable of forming a coordination bond with copper which enhances the adsorption of the compounds on the metal surface. It is apparent that the adsorption of these oxadiazole derivatives on the brass surface could occur directly on the basis of donor

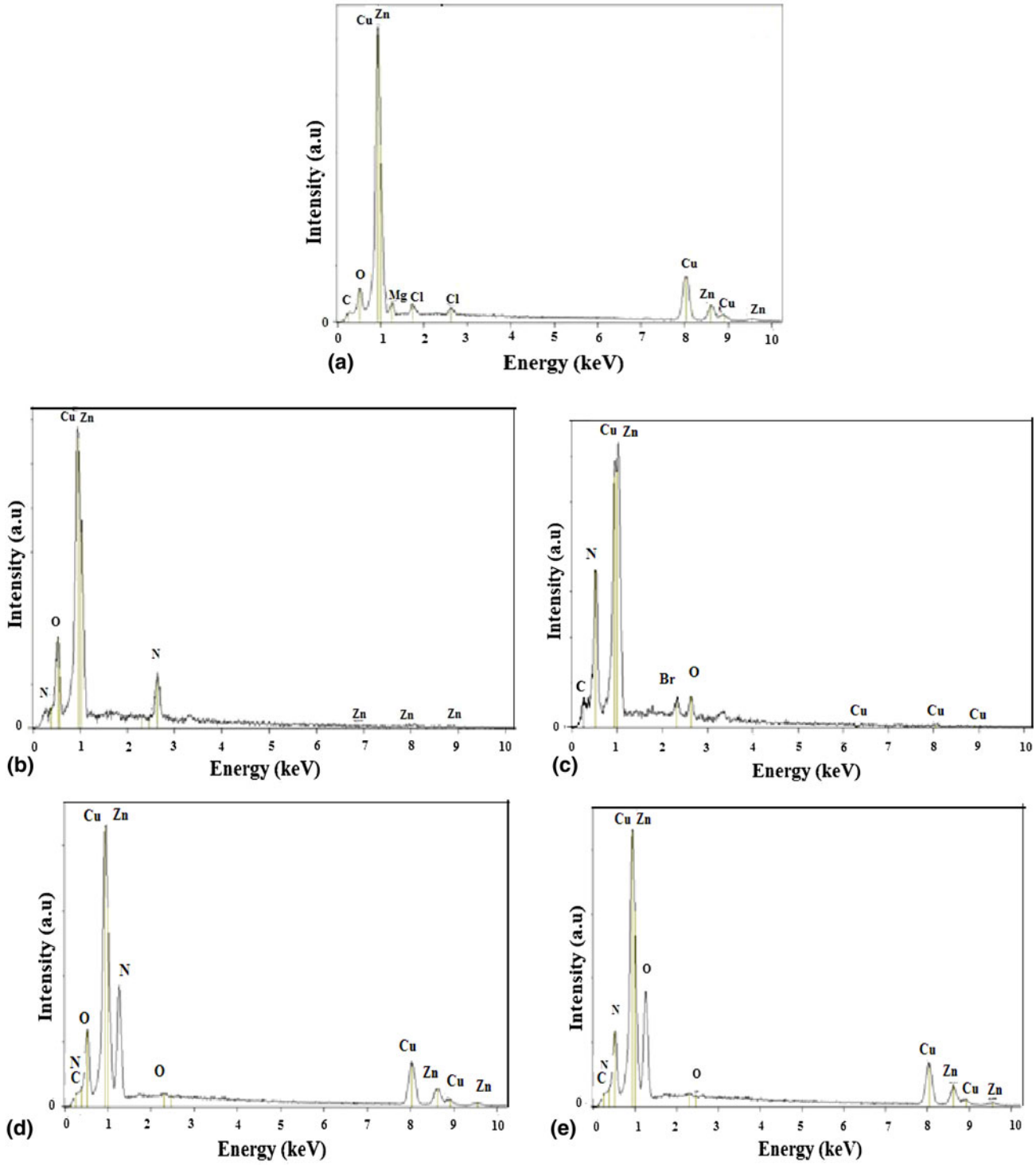

Fig. 8 EDX profile for brass surface (a) blank, (b) BAPOD, (c) BBPOD, (d) DPOD, and (e) BNPOD

behavior of the hetero atoms bearing the lone pair of electrons and the extensively delocalized π-electrons of the inhibitor molecules with the acceptor behavior of the vacant *d*-orbitals of brass surface atoms. The BAPOD was found to give excellent inhibition due to the presence of additional electron donating group ($-NH_2$) on the oxadiazole derivative which increases the electron density. This leads to the strong electrostatic attraction of BAPOD on the metal surface thereby resulting in the high inhibition efficiency. The better inhibition performance of BAPOD and BBPOD is due to the presence of electron donating amino and bromo groups, respectively, in their structures which increase the electron density of the aromatic ring and makes the π-electrons more available to interact with brass surface. Thus, BAPOD, BBPOD, and DPOD are more effectively adsorbed on the brass surface. However, the poor performance of the BNPOD may be attributed to the presence NO_2 group in it. The nitro group is a strong electron withdrawing group and thus it reduces the π-electron density

of the aromatic ring and the availability of π-electrons for interaction with brass is decreased. The inhibition efficiency of the oxadiazole derivatives for brass follows the order BAPOD > BBPOD > DPOD ≫ BNPOD.

4. Conclusions

The corrosion behavior of brass was investigated by electrochemical measurements in natural seawater in the absence and presence of various concentrations of oxadiazole derivatives such as BAPOD, BBPOD, DPOD, and BNPOD at different temperatures. From the results, it is suggested that compounds BAPOD, BBPOD, and DPOD show good inhibiting properties that increases with inhibitor concentration except BNPOD which gives insignificant inhibition efficiency with increasing the concentration due to the presence of electron withdrawing nitro group. Electrochemical impedance spectroscopic measurements indicated that the inhibitors hinder the corrosion process due to the increase of charge-transfer resistance, film resistance, and faradaic resistance related to the stabilization of adsorbed films. Surface morphological studies such as FT-IR, SEM, and EDX analysis showed that a film of inhibitor was formed on the brass surface. The film inhibited the growth of oxides of copper and zinc. ICP-AES analysis revealed that the investigated inhibitors effectively control the dezincification of brass.

Acknowledgments

One of the authors X. Joseph Raj acknowledges the University Grant Commission (UGC), New Delhi for financial assistance.

References

1. M.G. Fontana, *Corrosion Engineering*, 3rd ed., McGraw-Hill, New York, 1986, p 86
2. H.M. Shalaby, A. Al-Hashem, M. Lowther, and J. Al-Besharah, Ed., *Industrial Corrosion and Corrosion Control Technology*, Kuwait Institute for Scientific Research, Kuwait, 1996
3. A. El Warraky, H.A. El Shayeb, and E.M. Sherif, Pitting Corrosion of Copper in Chloride Solutions, *Anti-Corros. Methods Mater.*, 2004, **51**, p 52–61
4. E.M. Sherif and S.M. Park, Inhibition of Copper Corrosion in Acidic Pickling Solutions by N-phenyl-1,4-Phenylenediamine, *Electrochim. Acta*, 2006, **51**, p 4665–4673
5. S.M. Milic and M.M. Antonijevic, Some Aspects of Copper Corrosion in Presence of Benzotriazole and Chloride Ions, *Corros. Sci.*, 2009, **51**, p 28–34
6. J.M. Bastidas, P. Pinilla, E. Cano, J.L. Polo, and S. Miguel, Copper Corrosion Inhibition by Triphenylmethane Derivatives in Sulphuric Acid Media, *Corros. Sci.*, 2003, **45**, p 427–449
7. L.M. Rodrıguez-Valdez, A. Martınez-Villafane, and D. Glossman-Mitnik, Computational Studies on Glyceraldehyde and Glycine Maillard Reaction-II, *J. Mol. Struct. (Theochem)*, 2005, **713**, p 65–71
8. F. Bentiss, M. Traisnel, and M. Lagrene, Influence of 2, 5-Bis(4-Dimethylaminophenyl)-1,3,4-Thiadiazole on Corrosion Inhibition of Mild Steel in Acidic Media, *J. Appl. Electrochem.*, 2001, **31**, p 41–48
9. R. Ravichandran, S. Nanjundan, and N. Rajendran, Corrosion Inhibition of Brass by Benzotriazole Derivatives in NaCl Solution, *Anti-Corros. Methods Mater.*, 2005, **52**, p 226–232
10. R. Ravichandran and N. Rajendran, Influence of Benzotriazole Derivatives on the Dezincification of 65-35 Brass in Sodium Chloride, *Appl. Surf. Sci.*, 2005, **239**, p 182–192
11. R. Ravichandran, S. Nanjundan, and N. Rajendran, Effect of Benzotriazole Derivatives on the Corrosion of Brass in NaCl Solutions, *Appl. Surf. Sci.*, 2004, **236**, p 241–250
12. R. Ravichandran, S. Nanjundan, and N. Rajendran, Effect of Benzotriazole Derivatives on the Corrosion and Dezincification of Brass in Neutral Chloride Solution, *J. Appl. Electrochem.*, 2004, **34**, p 1171–1176
13. R. Ravichandran and N. Rajendran, Electrochemical Behaviour of Brass in Artificial Seawater. Effect of Organic Inhibitors, *Appl. Surf. Sci.*, 2005, **241**, p 449–458
14. A.P. Pchelnikov, A.D. Sitnikov, I.K. Marshakov, and V.V. Losev, A Study of the Kinetics and Mechanism of Brass Dezincification by Radiotracer and Electrochemical Methods, *Electrochim. Acta*, 1981, **29**, p 591–600
15. K. Samardzija, C. Lupu, N. Hackerman, A.R. Barron, and A. Luttge, Inhibitive Properties and Surface Morphology of a Group of Heterocyclic Diazoles as Inhibitors for Acidic Iron Corrosion, *Langmuir*, 2005, **21**, p 12187–12196
16. H.O. Curkovic, E. Stupnisek-Lisac, and H. Takenouti, The Influence of pH Value on the Efficiency of Imidazole Based Corrosion Inhibitors of Copper, *Corros. Sci.*, 2010, **52**, p 398–405
17. S. Varvara, L.M. Muresan, K. Rahmouni, and H. Takenouti, Evaluation of Some Non-toxic Thiadiazole Derivatives as Bronze Corrosion Inhibitors in Aqueous Solution, *Corros. Sci.*, 2008, **50**, p 2596–2604
18. H.O. Curkovic, E. Stupnisek-Lisac, and H. Takenouti, Electrochemical Quartz Crystal Microbalance and Electrochemical Impedance Spectroscopy Study of Copper Corrosion Inhibition by Imidazoles, *Corros. Sci.*, 2009, **51**, p 2342–2348
19. P. Galicia, N. Batina, and I. Gonzalez, The Relationship Between the Surface Composition and Electrical Properties of Corrosion Films Formed on Carbon Steel in Alkaline Sour Medium: An XPS and EIS Study, *J. Phys. Chem. B*, 2006, **110**, p 14398–14405
20. K. Babic-Samardzija, K.F. Khaled, and N. Hackerman, Investigation of the Inhibiting Action of O-, S- and N-Dithiocarbamato(1, 4, 8, 11-Tetraazacyclotetradecane)Cobalt(III) Complexes on the Corrosion of Iron in $HClO_4$ Acid, *Appl. Surf. Sci.*, 2005, **240**, p 327–340
21. H.H. Hassan, E. Abdelghani, and M.A. Amin, Inhibition of Mild Steel Corrosion in Hydrochloric Acid Solution by Triazole Derivatives: Part I. Polarization and EIS Studies, *Electrochim. Acta*, 2007, **52**, p 6359–6366
22. M. Lebrini, F. Bentiss, H. Vezin, and M. Lagrenee, The Inhibition of Mild Steel Corrosion in Acidic Solutions by 2,5-Bis(4-Pyridyl)-1,3,4-Thiadiazole: Structure-Activity Correlation, *Corros. Sci.*, 2006, **48**, p 1279–1291
23. A.M. Amin, Weight Loss Polarization, Electrochemical Impedance Spectroscopy, SEM and EDX Studies of the Corrosion Inhibition of Copper in Aerated NaCl Solutions, *J. Appl. Electrochem.*, 2006, **36**, p 215–226
24. H.S. Hegazy, E.A. Ashour, and B.G. Ateya, Effect of Benzotriazole on the Corrosion of Alpha Brass in Sulfide Polluted Saltwater, *J. Appl. Electrochem.*, 2001, **31**, p 1261–1265